Hindawi
Discrete Dynamics in Nature and Society
Volume 2023, Article ID 5894459, 17 pages
https://doi.org/10.1155/2023/5894459

Research Article

Fractional Derivative Model for Analysis of HIV and Malaria Transmission Dynamics

Kumama Regassa Cheneke [1,2]

[1]*Hawassa College of Teacher Education, Department of Mathematics, Hawassa, Ethiopia*
[2]*Wollega University, Department of Mathematics, Nekemte, Ethiopia*

Correspondence should be addressed to Kumama Regassa Cheneke; kumamaregassa@gmail.com

Received 27 April 2023; Revised 25 September 2023; Accepted 27 September 2023; Published 16 October 2023

Academic Editor: Chen Mengxin

In this study, a Caputo fractional derivative is employed to develop a model of malaria and HIV transmission dynamics with optimal control. Also, the model's basic properties are shown, and the basic reproduction number is computed using the next-generation matrix method. Additionally, the order of fractional derivative analysis shows that the infected group decreases at the beginning for the higher-order of fractional derivative. Moreover, the early activation of memory effects through public health education reduces the impact of malaria and HIV infections on further progression and transmission. On the other hand, effective optimal controls reduce the occurrence and prevalence of HIV and malaria infections from the beginning to the end of the investigation. Finally, the numerical simulations are done for the justification of analytical solutions with numerical solutions of the model. Moreover, the MATLAB platform is incorporated for numerical simulation of the solutions.

1. Introduction

Human immunodeficiency virus (HIV) is a human harmful virus that causes a fatal disease called acquired immunodeficiency syndrome (AIDS) [1]. There is no medication that cures AIDS disease, but effective antiretroviral (ARV) drugs could control the transmission and progression of the infection. HIV can be prevented using the prominent rule stated as abstinence-be-faithful-use-condom which is abbreviated as ABC rule. HIV can be transmitted to individuals through contact of fluids with HIV exposed objects. HIV can be transmitted vertically from mother to child and horizontally from person to person in an unsafe exposure to HIV exposed environment. Unsafe sexual practice is one of the major modes of HIV transmission. Malaria infection is a curable infection caused by a parasite called Plasmodium if the infected mosquito bites humans to suck the blood [2]. Globally, the consequence of deforestation is causing an increase in global warming that facilitates the risk of malaria infection. In the most part of sub-Saharan Africa, malaria cases and deaths are largely visible. The malaria and HIV diseases are studied separately for a long period of time as fatal diseases. However, the co-infection of HIV and malaria killed about 2 million each year [1].

Recently, mathematical models have become indispensable tools to describe the transmission and progression dynamics of disease in the human population [3–11]. The first mathematical model of malaria transmission dynamics is introduced by Ross [7]. Then, different mathematical models are constructed to describe transmission dynamics of malaria infection. Ngwa and Shu developed the malaria model with variable human and mosquito population [9]. Chitins et al. [10, 11] studied the transmission of malaria, considering that human and vector species follow a logistic population. They also studied the bifurcation analysis and the effects of seasonality that facilitate the spreading of the mosquito and feeding on the host. Li [8] studied the transmission of malaria through the stage-structured model and provides a basic analysis that shows backward bifurcation.

Boukhouima et al. [12, 13] studied the dynamics of virus in the human body through a fractional derivative. Hattaf

[14] developed the new generalized fractional derivative and applied it to the analysis of HIV dynamics in the body. Wu et al. [15] studied the cellular dynamics of the HIV-1 with uncertainty in the initial data. Dokuyucu and Dutta [16] studied the TB-HIV dynamics with the fractional order derivative. The order of the fractional derivative contributes to the memory effects. Okyere et al. [17] studied the transmission dynamics of malaria using the optimal fractional order derivative. Okyere et al. [18] studied the invasion of disease in the ecological population, whereas the diffusive model of COVID-19 is studied in [19]. As a basis for the memory effect, awareness intervention has contributed to reducing disease transmission [20]. In addition, the work done in [21–31] can be used to illustrate how mathematical models have recently played a part in providing information for the public through fitting data and new methods. In addition, in [31–34], co-infection models are constructed to describe the dynamics of HIV, cholera, and COVID-19 infections. Although some models are developed to study the dynamics of HIV and malaria, the fractional order derivative is incorporated to study the co-dynamics of malaria and HIV transmission dynamics. In this study, we are motivated by the works done in [1] and extend it to the fractional derivative model.

In addition, the remaining portions of the work are organized as follows. Section 2 discusses the creation of the mathematical model. Section 3 presents a basic analysis of the model without control. Section 4 presents the optimal control problem. Numerical simulation is presented in Section 5. Results and discussions are presented in Section 6. The conclusion is presented in Section 7.

2. Mathematical Model Formulation

In this study, the total population is classified into compartments as follows: (i) susceptible (S): It consists of all human who are infection-free and have a chance to be infected in the future; (ii) malaria-infected (I_m): This consists of only malaria-infected individuals; (iii) HIV-infected: It consists of only HIV-infected individuals; (iv) HIV-malaria-infected: It consists of all individuals infected with both malaria and HIV infections before the AIDS stage; (v) AIDS patients: It consists of individuals infected with HIV at the AIDS stage; (vi) AIDS-malaria-infected: It consists of individuals infected with malaria at the AIDS stage; (vii) susceptible mosquito (S_v): It consists of non-infectious mosquito population with chance to become infectious if they suck the blood of malaria infected human individuals; and (viii) infectious mosquito (I_v): It consists of infectious mosquito vector.

Moreover, the state variables and parameters used in the model are described in Tables 1 and 2, respectively.

Considering the structural representation given in Figure 1, we have constructed the fractional model for HIV and malaria transmission dynamics without control as given by the following equation:

$$\begin{aligned}
{}_0^C D_t^\alpha S &= \Lambda_h - \beta_h S(I_h + I_{hm} + I_a + I_{am}) - \beta_m S I_v - \mu S,\\
{}_0^C D_t^\alpha I_m &= \beta_m S I_v - \beta_h I_m\,(I_h + I_{hm} + I_a + I_{am}) - (\delta_m + \mu) I_m,\\
{}_0^C D_t^\alpha I_h &= \beta_h S(I_h + I_{hm} + I_a + I_{am}) - \beta_m I_h I_v - \eta I_h - \mu I_h,\\
{}_0^C D_t^\alpha I_{hm} &= \beta_m I_h I_v + \beta_h I_m\,(I_h + I_{hm} + I_a + I_{am}) - \xi I_{hm} - \delta_{hm} I_{hm} - \mu I_{hm},\\
{}_0^C D_t^\alpha I_a &= \eta I_h - \beta_m I_a I_v - \delta_a I_a - \mu I_a,\\
{}_0^C D_t^\alpha I_{am} &= \beta_m I_a I_v + \xi I_{hm} - \delta_{am} I_{am} - \mu I_{am},\\
{}_0^C D_t^\alpha S_v &= \Lambda_v - \beta_v S_v(I_m + I_{hm} + I_{am}) - \nu S_v,\\
{}_0^C D_t^\alpha I_v &= \beta_v S_v(I_m + I_{hm} + I_{am}) - \nu I_v,
\end{aligned} \tag{1}$$

with initial conditions $S(0) \geq 0, I_m(0) \geq 0, I_h(0) \geq 0, I_{hm}(0) \geq 0, I_a(0) \geq 0, I_{am}(0) \geq 0, S_v(0) \geq 0, I_v(0) \geq 0$.

3. Mathematical Analysis of the Model

3.1. Invariant Region

Theorem 1. *The solution of Caputo fractional derivative model (1) is invariant in the invariant set $\Omega \subset \mathfrak{R}_+^6 \times \mathfrak{R}_+^2$ such that*

$$\Omega = \Omega_h \times \Omega_v = \left\{(S, I_m, I_h, I_{hm}, I_a, I_{am}, S_v, I_v) \in \mathfrak{R}_+^6 \times \mathfrak{R}_+^2 \colon N_h \leq \frac{\Lambda_h}{\mu}, N_m \leq \frac{\Lambda_v}{\nu}\right\}, \tag{2}$$

Table 1: State variable and description.

State variable	Description
$S(t)$	Size of susceptible human individuals
$I_m(t)$	Size of malaria-infected human individuals
$I_h(t)$	Size of HIV-infected human individuals
$I_{hm}(t)$	Size of HIV- and malaria-infected human individuals
$I_a(t)$	Size of AIDS patients
$I_{am}(t)$	Size of AIDS- and malaria-infected individuals
$S_v(t)$	Size of susceptible mosquito
$I_v(t)$	Size of infectious mosquito population

Table 2: Parameter and assigned value.

Parameter	Value
Λ_h	Recruitment rate of susceptible human individuals
β_h	Transmission rate of HIV infection
β_m	Transmission rate of malaria infection
μ	Natural death rate of all human individuals
δ_m	Malaria-induced death rate
η	Progression rate from I_h to I_a
ξ	Transfer rate from I_{hm} to I_{am}
δ_{am}	AIDS-malaria induced death rate
δ_{hm}	HIV-malaria induced death rate
δ_a	AIDS-induced death rate
Λ_v	Recruitment rate of susceptible mosquito
β_v	Transmission rate of malaria from infected mosquito
ν	Death rate of mosquito individuals
γ	Treatment rate of malaria-infected
ω	Treatment rate of AIDS-malaria-infected
ρ	Treatment rate of HIV-malaria-infected

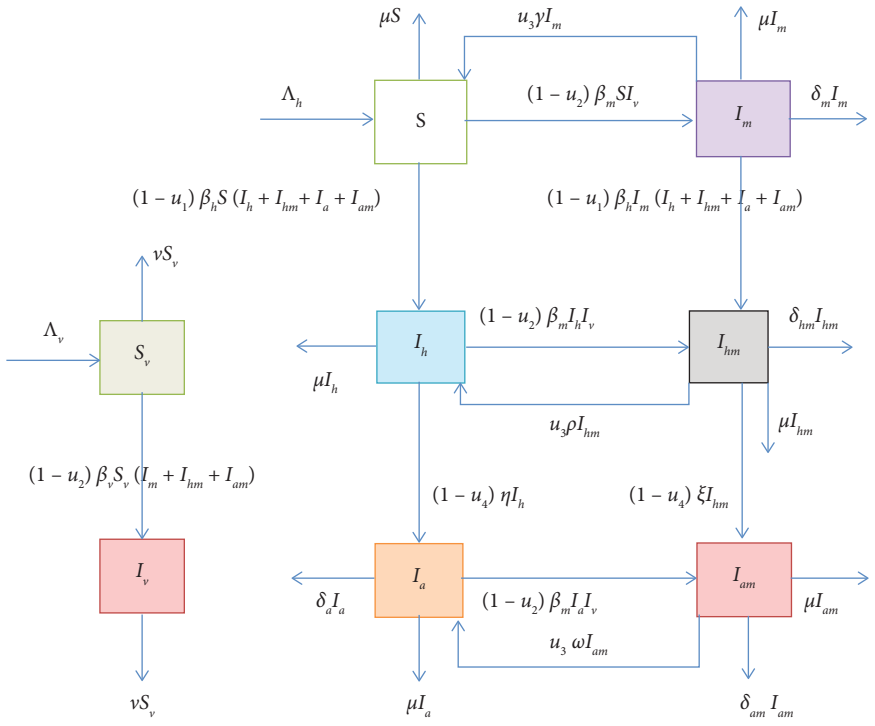

Figure 1: Architecture of HIV and malaria transmission dynamics.

where $N_h = S + I_m + I_h + I_a + I_{am}, N_m = S_v + I_v$.

Proof. Considering the human population equation and adding the right and left expressions of the fractional derivative part gives

$$ {}_0^C D_t^\alpha N_h = \Lambda_h - \mu N_h - \delta_m I_m - \delta_{hm} I_{hm} - \delta_a I_a - \delta_{am} I_{am}, \tag{3} $$

which implies

$$ {}_0^C D_t^\alpha N_h \le \Lambda_h - \mu N_h. \tag{4} $$

Applying the Laplace transform on both sides and solving the preceding expression as t reaches infinity, we obtain

$$ N_h \le \frac{\Lambda_h}{\mu} - \left(\frac{\Lambda_h}{\mu} - N_h(0) \right) E_{\alpha,1}(-\mu t). \tag{5} $$

Hence, the solution of the developed is bounded for all time t. □

3.2. Non-Negativity of Solution

Theorem 2. *The solution of Caputo fractional derivative model (1) is non-negative in the invariant region for all time t.*

Proof. To show the non-negativity of solution, consider model (1) along the axis where state variables vanish as follows:

$$ \begin{aligned} {}_0^C D_t^\alpha S\big|_{S=0} &= \Lambda_h \ge 0, \\ {}_0^C D_t^\alpha I_m\big|_{I_m=0} &= \beta_m S I_v \ge 0, \\ {}_0^C D_t^\alpha I_h\big|_{I_h=0} &= \beta_h S (I_{hm} + I_a + I_{am}) \ge 0, \\ {}_0^C D_t^\alpha I_{hm}\big|_{I_{hm}=0} &= \beta_m I_h I_v + \beta_h I_m (I_h + I_a + I_{am}) \ge 0, \\ {}_0^C D_t^\alpha I_a\big|_{I_a=0} &= \eta I_h \ge 0, \\ {}_0^C D_t^\alpha I_{am}\big|_{I_{am}=0} &= \beta_m I_a I_v + \xi I_{hm} \ge 0, \\ {}_0^C D_t^\alpha S_v\big|_{S_v=0} &= \Lambda_v \ge 0, \\ {}_0^C D_t^\alpha I_v\big|_{I_v=0} &= \beta_v S_v (I_m + I_{hm} + I_{am}) \ge 0. \end{aligned} \tag{6} $$

Hence, by Caputo generalized mean value theorem, the solution of constructed model is non-negative. □

3.3. Existence and Uniqueness of Solutions

Theorem 3. *The solution of Caputo fractional derivative model (1) exists and is unique in the defined invariant region Ω.*

Proof. The proof can be shown using the fixed point theory [5]. □

3.4. Disease-Free Equilibrium.

The disease-free equilibrium E_0^C of Caputo fractional derivative model (1) is a steady state point of disease extinction. It is computed and given by

$$ E_0^C = \left(\frac{\Lambda_h}{\mu}, \ 0, \ 0, \ 0, \ 0, \ 0, \ \frac{\Lambda_v}{\nu}, \ 0 \right). \tag{7} $$

3.5. Basic Reproduction Number.

The basic reproduction number (R_0) is extensively applied in mathematical epidemiology to describe the status of infections invading the population. The biological significance of basic reproduction number is that it shows the status of the disease in the population, whether the disease in the population is extinct if $R_0 < 1$ or persists if $R_0 > 1$ [35–37]. Recently, a next-generation matrix method is broadly incorporated in the modern research on infections transmission dynamics. Here also, similar to the works done in [35–37], we have applied the next-generation matrix to compute the basic reproduction number. Hence, from model (1), we construct a matrix f that comprises of newly infected individuals arriving in the compartments, and a matrix v encompasses the transition terms in the infected compartments.

First, from only the malaria model, we construct basic reproduction using the subsequent vectors.

$$ \begin{aligned} f &= \begin{pmatrix} \beta_m S I_v \\ \beta_v S_v I_m \end{pmatrix}, \\ v &= \begin{pmatrix} (\delta_m + \mu) I_m \\ \nu I_v \end{pmatrix}. \end{aligned} \tag{8} $$

At disease-free equilibrium, the Jacobian matrices F and V obtained from preceding vectors f and v, respectively, are given by

$$ \begin{aligned} F &= \begin{pmatrix} 0 & \beta_m S \\ \beta_v S_v & 0 \end{pmatrix}, \\ V &= \begin{pmatrix} \delta_m + \mu & 0 \\ 0 & \nu \end{pmatrix}. \end{aligned} \tag{9} $$

The next-generation matrix FV^{-1} is constructed from the preceding matrices F and V as follows:

$$ FV^{-1} = \begin{pmatrix} 0 & \dfrac{\beta_m S}{\nu} \\ \dfrac{\beta_v S_v}{\delta_m + \mu} & 0 \end{pmatrix}. \tag{10} $$

The eigenvalues of the next-generation matrix FV^{-1} are computed as follows:

$$ \begin{aligned} \lambda_1 &= \frac{\sqrt{\beta_m}\sqrt{\beta_v}\sqrt{S}\sqrt{S_v}}{\sqrt{\nu}\sqrt{\delta_m + \mu}}, \\ \lambda_2 &= -\frac{\sqrt{\beta_m}\sqrt{\beta_v}\sqrt{S}\sqrt{S_v}}{\sqrt{\nu}\sqrt{\delta_m + \mu}}. \end{aligned} \tag{11} $$

Furthermore, the basic reproduction number R_{0m} is the spectral radius of next-generation matrix FV^{-1}. Hence, we have

$$\begin{aligned} R_{0m} &= \rho\left(FV^{-1}\right) \\ &= \frac{\sqrt{\beta_m}\sqrt{\beta_v}\sqrt{S^0}\sqrt{S_v}}{\sqrt{\nu}\sqrt{\delta_m+\mu}}. \end{aligned} \tag{12}$$

Second, from only the malaria model, we construct basic reproduction using the subsequent vectors.

$$\begin{aligned} f &= \begin{pmatrix} \beta_h S(I_h + I_a) \\ 0 \end{pmatrix}, \\ v &= \begin{pmatrix} \eta I_h + \mu I_h \\ -\eta I_h + \delta_a I_a + \mu I_a \end{pmatrix}. \end{aligned} \tag{13}$$

At disease-free equilibrium, the Jacobian matrices F and V obtained from preceding vectors f and v, respectively, are given by

$$\begin{aligned} F &= \begin{pmatrix} \beta_h S^0 & \beta_h S^0 \\ 0 & 0 \end{pmatrix}, \\ V &= \begin{pmatrix} \eta+\mu & 0 \\ -\eta & \delta_a+\mu \end{pmatrix}. \end{aligned} \tag{14}$$

The next-generation matrix FV^{-1} is constructed from the preceding matrices F and V as follows:

$$FV^{-1} = \begin{pmatrix} \dfrac{\beta_h S^0}{\eta+\mu} + \dfrac{\beta_h S^0 \eta}{(\delta+\mu)(\eta+\mu)} & \dfrac{\beta_h S^0}{\delta+\mu} \\ 0 & 0 \end{pmatrix}. \tag{15}$$

The eigenvalues of the next-generation matrix FV^{-1} are computed as follows:

$$\begin{aligned} \lambda_1 &= \frac{\beta_h S^0}{\eta+\mu} + \frac{\beta_h S^0 \eta}{(\delta+\mu)(\eta+\mu)}, \\ \lambda_2 &= 0. \end{aligned} \tag{16}$$

Furthermore, the basic reproductions number R_{0h} is the spectral radius of next-generation matrix FV^{-1}. Hence, we have

$$\begin{aligned} R_{0h} &= \rho\left(FV^{-1}\right) \\ &= \frac{\beta_h S^0}{\eta+\mu} + \frac{\beta_h S^0 \eta}{(\delta+\mu)(\eta+\mu)}. \end{aligned} \tag{17}$$

Moreover, according to the works done in [1], the basic reproduction number R_0 of the full model (1) is given by

$$\begin{aligned} R_0 &= \max\left\{ \frac{\sqrt{\beta_m}\sqrt{\beta_v}\sqrt{S^0}\sqrt{S_v}}{\sqrt{\nu}\sqrt{\delta_m+\mu}}, \frac{\beta_h S^0}{\eta+\mu} + \frac{\beta_h S^0 \eta}{(\delta+\mu)(\eta+\mu)} \right\} \\ &= \max\{R_{0m}, R_{0h}\}. \end{aligned} \tag{18}$$

3.6. Global Stability of Disease-Free Equilibrium

Theorem 4. *The disease-free equilibrium E_0 of fractional model is globally asymptotically stable if $R_0 \le 1$ and unstable if $R_0 > 1$.*

Proof. To show global stability, we follow the works of Castillo–Chavez and Song done in [2]. Now, we consider the infected compartments of model (1) as given below. First, let X be vector of variables for infection-free compartments and Y be vector of infected compartments such that

$$G(X,Y) = \begin{pmatrix} -\delta_m-\mu & 0 & 0 & 0 & 0 & 0 \\ 0 & -\eta-\mu & 0 & 0 & 0 & 0 \\ 0 & 0 & -\xi-\delta_{hm}-\mu & 0 & 0 & 0 \\ 0 & \eta & 0 & -\delta_a-\mu & 0 & 0 \\ 0 & 0 & \xi & 0 & -\delta_{am}-\mu & 0 \\ 0 & 0 & 0 & 0 & 0 & -\nu \end{pmatrix} \begin{pmatrix} I_m \\ I_h \\ I_{hm} \\ I_a \\ I_{am} \\ I_v \end{pmatrix} - \begin{pmatrix} 0 \\ 0 \\ 0 \\ 0 \\ 0 \\ 0 \end{pmatrix}, \tag{19}$$

which implies

$$G(X,Y) = PY - \widehat{G}(X,Y), \tag{20}$$

where the subsequent matrix is a Metzler matrix.

$$P = \begin{pmatrix} -\delta_m - \mu & 0 & 0 & 0 & 0 & 0 \\ 0 & -\eta - \mu & 0 & 0 & 0 & 0 \\ 0 & 0 & -\xi - \delta_{hm} - \mu & 0 & 0 & 0 \\ 0 & \eta & 0 & -\delta_a - \mu & 0 & 0 \\ 0 & 0 & \xi & 0 & -\delta_{am} - \mu & 0 \\ 0 & 0 & 0 & 0 & 0 & -\nu \end{pmatrix},$$
$$\widehat{G}(X,Y) = \begin{pmatrix} 0 \\ 0 \\ 0 \\ 0 \\ 0 \\ 0 \end{pmatrix}. \tag{21}$$

Hence, the conditions of Castillo–Chavez and song are satisfied. Therefore, the disease-free equilibrium of model (1) is globally asymptotically stable. □

4. Extension to Optimal Control Problem

In this section, we study the optimal control problem of HIV and malaria co-infection transmission dynamics for $\alpha = 1$. Since the optimal control problem is very methodical and hypothetical, it is applied in real life by taking feedback from the target community based on numerical solutions of model. Moreover, the control functions are taken in the study can be described as follows: (i) HIV prevention control (u_1): The intervention with this control reduces the chance of getting with HIV infections, (ii) malaria prevention control (u_2): This control function helps in the prevention of malaria infection, (iii) malaria treatment control (u_3): This control function is applied to treat individuals infected with malaria infection, (iv) HIV progression control (u_4): This is HIV treatment control function applied for slowing HIV infection to the advanced stage.

$$\begin{aligned}
\frac{dS}{dt} &= \Lambda_h - (1-u_1)\beta_h S(I_h + I_{hm} + I_a + I_{am}) - (1-u_2)\beta_m S I_v + u_3\gamma I_m - \mu S,\\
\frac{dI_m}{dt} &= (1-u_2)\beta_m S I_v - (1-u_1)\beta_h I_m (I_h + I_{hm} + I_a + I_{am}) - u_3\gamma I_m - (\delta_m + \mu) I_m,\\
\frac{dI_h}{dt} &= (1-u_1)\beta_h S(I_h + I_{hm} + I_a + I_{am}) + u_3\rho I_{hm} - (1-u_2)\beta_m I_h I_v - (1-u_4)\eta I_h - \mu I_h,\\
\frac{dI_{hm}}{dt} &= (1-u_2)\beta_m I_h I_v + (1-u_1)\beta_h I_m (I_h + I_{hm} + I_a + I_{am}) - u_3\rho I_{hm} - (1-u_4)\xi I_{hm} - \delta_{hm} I_{hm} - \mu I_{hm},\\
\frac{dI_a}{dt} &= (1-u_4)\eta I_h + u_3\omega I_{am} - (1-u_2)\beta_m I_a I_v - \delta_a I_a - \mu I_a,\\
\frac{dI_{am}}{dt} &= (1-u_2)\beta_m I_a I_v + (1-u_4)\xi I_{hm} - u_3\omega I_{am} - \delta_{am} I_{am} - \mu I_{am},\\
\frac{dS_v}{dt} &= \Lambda_v - (1-u_2)\beta_v S_v (I_m + I_{hm} + I_{am}) - \nu S_v,\\
\frac{dI_v}{dt} &= (1-u_2)\beta_v S_v (I_m + I_{hm} + I_{am}) - \nu I_v.
\end{aligned} \tag{22}$$

4.1. Objective Function. The objective functional for minimization of cost of using controls and the number of infected compartments is defined by

$$J = \min_{u_1,u_2,u_3,u_4} \int_0^{t_f} c_1 I_m + c_2 I_h + c_3 I_{hm} + c_4 I_a + c_5 I_{am} + c_6 I_v + \frac{1}{2}\left(\sum_{i=1}^{4} w_i u_i^2\right) \mathrm{d}t. \tag{23}$$

4.2. Hamiltonian Function. Pontryagin's maximum principle is applied for the construction of the Hamiltonian function that minimizes the objective function, as given by subsequent equation (38). Let $\lambda_i, i = 1, 2, 3, 4, 5, 6, 7, 8$ be adjoint variables corresponding to state variables $S, I_m, I_h, I_{hm}, I_a, I_{am}, S_v, I_v$, respectively. Hence, we define Hamiltonian function as follows:

$$\begin{aligned} H = {} & c_1 I_m + c_2 I_h + c_3 I_{hm} + c_4 I_a + c_5 I_{am} + c_6 I_v + \frac{1}{2}\left(\sum_{i=1}^{4} w_i u_i^2\right) + \lambda_1 \frac{\mathrm{d}S}{\mathrm{d}t} + \lambda_2 \frac{\mathrm{d}I_m}{\mathrm{d}t} + \lambda_3 \frac{\mathrm{d}I_h}{\mathrm{d}t} + \lambda_4 \frac{\mathrm{d}I_{hm}}{\mathrm{d}t} \\ & + \lambda_5 \frac{\mathrm{d}I_a}{\mathrm{d}t} + \lambda_6 \frac{\mathrm{d}I_{am}}{\mathrm{d}t} + \lambda_7 \frac{\mathrm{d}S_v}{\mathrm{d}t} + \lambda_8 \frac{\mathrm{d}I_v}{\mathrm{d}t}, \end{aligned} \tag{24}$$

which implies

$$\begin{aligned} H = {} & c_1 I_m + c_2 I_h + c_3 I_{hm} + c_4 I_a + c_5 I_{am} + c_6 I_v + \frac{1}{2}\left(\sum_{i=1}^{4} w_i u_i^2\right) \\ & + \lambda_1 \left[\Lambda_h - (1-u_1)\beta_h S(I_h + I_{hm} + I_a + I_{am}) - (1-u_2)\beta_m S I_v + u_3 \gamma I_m - \mu S\right] \\ & + \lambda_2 \left[(1-u_2)\beta_m S I_v - (1-u_1)\beta_h I_m (I_h + I_{hm} + I_a + I_{am}) - u_3 \gamma I_m - (\delta_m + \mu) I_m\right] \\ & + \lambda_3 \left[(1-u_1)\beta_h S(I_h + I_{hm} + I_a + I_{am}) + u_3 \rho I_{hm} - (1-u_2)\beta_m I_h I_v - (1-u_4)\eta I_h - \mu I_h\right] \\ & + \lambda_4 \left[(1-u_2)\beta_m I_h I_v + (1-u_1)\beta_h I_m (I_h + I_{hm} + I_a + I_{am}) - u_3 \rho I_{hm} - (1-u_4)\xi I_{hm} - \delta_{hm} I_{hm} - \mu I_{hm}\right] \\ & + \lambda_5 \left[(1-u_4)\eta I_h + u_3 \omega I_{am} - (1-u_2)\beta_m I_a I_v - \delta_a I_a - \mu I_a\right] + \lambda_6 \left[(1-u_2)\beta_m I_a I_v + (1-u_4)\xi I_{hm} - u_3 \omega I_{am}\right. \\ & \left. - \delta_{am} I_{am} - \mu I_{am}\right] + \lambda_7 \left[\Lambda_v - (1-u_2)\beta_v S_v (I_m + I_{hm} + I_{am}) - \nu S_v\right] + \lambda_8 \left[(1-u_2)\beta_v S_v (I_m + I_{hm} + I_{am}) - \nu I_v\right]. \end{aligned} \tag{25}$$

4.3. Adjoint Equations. The adjoint equations are computed from the subsequent partial derivatives, that is,

$$\frac{d\lambda_1}{dt} = -\frac{\partial H}{\partial S}, \ \frac{d\lambda_2}{dt} = -\frac{\partial H}{\partial I_m}, \ \frac{d\lambda_3}{dt} = -\frac{\partial H}{\partial I_h}, \ \frac{d\lambda_4}{dt} = -\frac{\partial H}{\partial I_{hm}}, \ \frac{d\lambda_5}{dt} = -\frac{\partial H}{\partial I_a}, \ \frac{d\lambda_6}{dt} = -\frac{\partial H}{\partial I_{am}}, \ \frac{d\lambda_7}{dt} = -\frac{\partial H}{\partial I_m}, \ \frac{d\lambda_8}{dt} = -\frac{\partial H}{\partial I_v}. \tag{26}$$

Therefore, the adjoint equations are computed as follows:

$$\begin{aligned}
\frac{d\lambda_1}{dt} &= (1-u_1)\beta_h(I_h + I_{hm} + I_a + I_{am})(\lambda_1 - \lambda_3) + (1-u_2)\beta_m I_v(\lambda_1 - \lambda_2) + \mu\lambda_1,\\
\frac{d\lambda_2}{dt} &= -c_1 + (1-u_1)\beta_h(I_h + I_{hm} + I_a + I_{am})(\lambda_2 - \lambda_4) + u_3\gamma(\lambda_2 - \lambda_1) + (1-u_2)\beta_v S_v(\lambda_7 - \lambda_8) + (\delta_m + \mu)\lambda_2,\\
\frac{d\lambda_3}{dt} &= -c_2 + (1-u_1)\beta_h S(\lambda_1 - \lambda_3) + (1-u_1)\beta_h I_m(\lambda_2 - \lambda_4) + (1-u_2)\beta_m I_v(\lambda_3 - \lambda_4) + (1-u_4)\eta(\lambda_3 - \lambda_5) + \mu\lambda_3,\\
\frac{d\lambda_4}{dt} &= -c_3 + (1-u_1)\beta_h S(\lambda_1 - \lambda_3) + (1-u_1)\beta_h I_m(\lambda_2 - \lambda_4) + u_3\rho(\lambda_4 - \lambda_3) + (1-u_4)\xi(\lambda_4 - \lambda_6)\\
&\quad + (1-u_2)\beta_v S_v(\lambda_7 - \lambda_8) + (\delta_{hm} + \mu)\lambda_4,\\
\frac{d\lambda_5}{dt} &= -c_4 + (1-u_1)\beta_h S(\lambda_1 - \lambda_3) + (1-u_1)\beta_h I_m(\lambda_2 - \lambda_4) + (1-u_2)\beta_m I_v(\lambda_5 - \lambda_6) + \lambda_5(\delta_a + \mu),\\
\frac{d\lambda_6}{dt} &= -c_5 + (1-u_1)\beta_h S(\lambda_1 - \lambda_3) + (1-u_1)\beta_h I_m(\lambda_2 - \lambda_4) + u_3\omega(\lambda_6 - \lambda_5) + (1-u_2)\beta_v S_v(\lambda_7 - \lambda_8) + (\delta_{am} + \mu)\lambda_8,\\
\frac{d\lambda_7}{dt} &= (1-u_2)\beta_v(I_m + I_{hm} + I_{am})(\lambda_7 - \lambda_8) + \nu\lambda_7,\\
\frac{d\lambda_8}{dt} &= -c_6 + (1-u_2)\beta_m S(\lambda_1 - \lambda_2) + (1-u_2)\beta_m I_h(\lambda_3 - \lambda_4) + (1-u_2)\beta_m I_a(\lambda_5 - \lambda_6) + \nu\lambda_8,
\end{aligned} \tag{27}$$

with transversal conditions $\lambda_i(t_f) = 0, i = 1, 2, 3, 4, 5, 6, 7, 8$.

4.4. Optimal Control Functions. The optimal controls u_1^*, u_2^*, u_3^* and u_4^* are obtained by solving the subsequent equations.

$$\frac{\partial H}{\partial u_1} = 0, \frac{\partial H}{\partial u_2} = 0, \frac{\partial H}{\partial u_3} = 0, \frac{\partial H}{\partial u_4} = 0. \tag{28}$$

To obtain u_1^*, we solve, from the subsequent equation, for u_1.

$$\frac{\partial H}{\partial u_1} = 0. \tag{29}$$

The above implies

$$u_1 = \frac{\beta_h S(I_h + I_{hm} + I_a + I_{am})(\lambda_3 - \lambda_1) + \beta_h I_m(I_h + I_{hm} + I_a + I_{am})(\lambda_4 - \lambda_2)}{w_1} = u_1^*. \tag{30}$$

To obtain u_2^*, solve, from the subsequent equation, for u_2.

$$\frac{\partial H}{\partial u_2} = 0. \tag{31}$$

The above implies,

$$u_2 = \frac{\beta_m S I_v(\lambda_2 - \lambda_1) + \beta_m I_h I_v(\lambda_4 - \lambda_3) + \beta_m I_a I_v(\lambda_6 - \lambda_5) + \beta_v S_v(I_m + I_{hm} + I_{am})(\lambda_8 - \lambda_7)}{w_2} = u_2^*. \tag{32}$$

To obtain u_3^*, solve, from the subsequent equation, for u_3.

$$\frac{\partial H}{\partial u_3} = 0. \tag{33}$$

The above implies,

$$u_3 = \frac{\gamma I_m(\lambda_2 - \lambda_1) + \rho I_{hm}(\lambda_4 - \lambda_3) + \omega I_{am}(\lambda_6 - \lambda_5)}{w_3} = u_3^*. \tag{34}$$

To obtain u_4^*, solve, from the subsequent equation, for u_4.

$$\frac{\partial H}{\partial u_4} = 0. \tag{35}$$

The above implies,

$$u_4 = \frac{\xi I_{hm}(\lambda_6 - \lambda_4) + \eta I_h(\lambda_5 - \lambda_3)}{w_4} = u_4^*. \tag{36}$$

In compact form

$$\begin{aligned}
u_1^* &= \min\left\{1, \max\left\{0, \frac{\beta_h S(I_h + I_{hm} + I_a + I_{am})(\lambda_3 - \lambda_1) + \beta_h I_m (I_h + I_{hm} + I_a + I_{am})(\lambda_4 - \lambda_2)}{w_1}\right\}\right\},\\
u_2^* &= \min\left\{1, \max\left\{0, \frac{\beta_m S I_v(\lambda_2 - \lambda_1) + \beta_m I_h I_v(\lambda_4 - \lambda_3) + \beta_m I_a I_v(\lambda_6 - \lambda_5) + \beta_v S_v(I_m + I_{hm} + I_{am})(\lambda_8 - \lambda_7)}{w_2}\right\}\right\},\\
u_3^* &= \min\left\{1, \max\left\{0, \frac{\gamma I_m(\lambda_2 - \lambda_1) + \rho I_{hm}(\lambda_4 - \lambda_3) + \omega I_{am}(\lambda_6 - \lambda_5)}{w_3}\right\}\right\},\\
u_4^* &= \min\left\{1, \max\left\{0, \frac{\xi I_{hm}(\lambda_6 - \lambda_4) + \eta I_h(\lambda_5 - \lambda_3)}{w_4}\right\}\right\}.
\end{aligned} \tag{37}$$

4.4.1. Optimality System

$$\begin{aligned}
\frac{dS}{dt} &= \Lambda_h - (1-u_1)\beta_h S(I_h + I_{hm} + I_a + I_{am}) - (1-u_2)\beta_m S I_v + u_3\gamma I_m - \mu S,\\
\frac{dI_m}{dt} &= (1-u_2)\beta_m S I_v - (1-u_1)\beta_h I_m (I_h + I_{hm} + I_a + I_{am}) - u_3\gamma I_m - (\delta_m + \mu) I_m,\\
\frac{dI_h}{dt} &= (1-u_1)\beta_h S(I_h + I_{hm} + I_a + I_{am}) + u_3\rho I_{hm} - (1-u_2)\beta_m I_h I_v - (1-u_4)\eta I_h - \mu I_h,\\
\frac{dI_{hm}}{dt} &= (1-u_2)\beta_m I_h I_v + (1-u_1)\beta_h I_m (I_h + I_{hm} + I_a + I_{am}) - u_3\rho I_{hm} - (1-u_4)\xi I_{hm} - \delta_{hm} I_{hm} - \mu I_{hm},\\
\frac{dI_a}{dt} &= (1-u_4)\eta I_h + u_3\omega I_{am} - (1-u_2)\beta_m I_a I_v - \delta_a I_a - \mu I_a,\\
\frac{dI_{am}}{dt} &= (1-u_2)\beta_m I_a I_v + (1-u_4)\xi I_{hm} - u_3\omega I_{am} - \delta_{am} I_{am} - \mu I_{am},\\
\frac{dS_v}{dt} &= \Lambda_v - (1-u_2)\beta_v S_v(I_m + I_{hm} + I_{am}) - \nu S_v,\\
\frac{dI_v}{dt} &= (1-u_2)\beta_v S_v(I_m + I_{hm} + I_{am}) - \nu I_v,
\end{aligned}$$

$$
\begin{aligned}
\frac{d\lambda_1}{dt} &= (1-u_1)\beta_h(I_h + I_{hm} + I_a + I_{am})(\lambda_1 - \lambda_3) + (1-u_2)\beta_m I_v(\lambda_1 - \lambda_2) + \mu\lambda_1,\\
\frac{d\lambda_2}{dt} &= -c_1 + (1-u_1)\beta_h(I_h + I_{hm} + I_a + I_{am})(\lambda_2 - \lambda_4) + u_3\gamma(\lambda_2 - \lambda_1) + (1-u_2)\beta_v S_v(\lambda_7 - \lambda_8) + (\delta_m + \mu)\lambda_2,\\
\frac{d\lambda_3}{dt} &= -c_2 + (1-u_1)\beta_h S(\lambda_1 - \lambda_3) + (1-u_1)\beta_h I_m(\lambda_2 - \lambda_4) + (1-u_2)\beta_m I_v(\lambda_3 - \lambda_4) + (1-u_4)\eta(\lambda_3 - \lambda_5) + \mu\lambda_3,\\
\frac{d\lambda_4}{dt} &= -c_3 + (1-u_1)\beta_h S(\lambda_1 - \lambda_3) + (1-u_1)\beta_h I_m(\lambda_2 - \lambda_4) + u_3\rho(\lambda_4 - \lambda_3) + (1-u_4)\xi(\lambda_4 - \lambda_6)\\
&\quad + (1-u_2)\beta_v S_v(\lambda_7 - \lambda_8) + (\delta_{hm} + \mu)\lambda_4,\\
\frac{d\lambda_5}{dt} &= -c_4 + (1-u_1)\beta_h S(\lambda_1 - \lambda_3) + (1-u_1)\beta_h I_m(\lambda_2 - \lambda_4) + (1-u_2)\beta_m I_v(\lambda_5 - \lambda_6) + (\delta_a + \mu)\lambda_5,\\
\frac{d\lambda_6}{dt} &= -c_5 + (1-u_1)\beta_h S(\lambda_1 - \lambda_3) + (1-u_1)\beta_h I_m(\lambda_2 - \lambda_4) + u_3\omega(\lambda_6 - \lambda_5) + (1-u_2)\beta_v S_v(\lambda_7 - \lambda_8) + (\delta_{am} + \mu)\lambda_6,\\
\frac{d\lambda_7}{dt} &= (1-u_2)\beta_v(I_m + I_{hm} + I_{am})(\lambda_7 - \lambda_8) + \nu\lambda_7,\\
\frac{d\lambda_8}{dt} &= -c_6 + (1-u_2)\beta_m S(\lambda_1 - \lambda_2) + (1-u_2)\beta_m I_h(\lambda_3 - \lambda_4) + (1-u_2)\beta_m I_a(\lambda_5 - \lambda_6) + \nu\lambda_8.
\end{aligned}
\tag{38}
$$

5. Numerical Simulations

In this section, we have used the compacted fde12 function which is designed to solve Caputo fractional derivative [39]. MATLAB platform is used for numerical simulations of population size to describe effects on memory and applied control measures. The some of the constants used in the simulations are $w_1 = 20, w_2 = 50, w_3 = 60, w_4 = 70, c_1 = 20, c_2 = 15, c_3 = 10, c_4 = 5, c_5 = 2, c_6 = 2$. Moreover, the applied initial value of state variables are $S(0) = 50, I_m(0) = 100, I_h(0) = 50, I_{hm}(0) = 30, I_a(0) = 50, I_{am}(0) = 50, S_v(0) = 5000, I_v(0) = 100$ and parameters values are given in the subsequent Table 3.

6. Results and Discussion

The fractional derivative model and the optimal control problem are analyzed with the support of numerical simulations.

In Figure 2, the susceptible population size decrease with high order of fractional derivative for long period of time. In Figure 3, the numerical simulations show that the size of only malaria infected human population decrease with high order of fractional derivative at the beginning of simulations. However, after a few years, for long time of interval, the size of malaria infected population increase as the order of fractional derivative increase. Moreover, at the end of numerical simulation, there is an inclination that high order of fractional derivative reduces size of malaria infected population.

In Figure 4, at the beginning of simulations, for high order of fractional derivative the size of only HIV-infected population decreases. Moreover, the small value of fractional derivative reduces a little whereas the HIV-infected population size decrease and increase for high order of fractional derivative. In Figure 5, the high order of fractional derivative reduces HIV-malaria infected population size only at the beginning of infection. In Figure 6, AIDS individuals' size is low for high order of fractional derivative after some specified time span of simulation. In Figure 7, the high order of fractional derivative reduces the infected population in the beginning of simulation. Moreover, for long period of time the high order of fractional derivative increase the infected individuals.

In Figure 8, the size of susceptible mosquito population decreases with high order of fractional derivative starting from the beginning of simulation time. In Figure 9, at the beginning, the size of infected mosquito population decrease for high value of order of fractional derivative. In Figure 10, it is diagnosed that the size of malaria infected population decrease due to intervention with control measures.

In Figure 11, it is observed that the presence of applied controls reduces the size of HIV-infected population effectively at the beginning and at the end of simulations time. In Figure 12, HIV-malaria infected population size decrease with presence control intervention. In Figure 13, the size of AIDS population decreases due to interventions with control measures for all time of simulation. In Figure 14, the simulation results show that the intervention with applied optimal controls reduces the AIDS-malaria infected population size whereas in Figure 15, the number of infected mosquito population decrease with applied available controls. In general, the study demonstrates that early intervention to manage the dynamics of HIV and malaria transmission by prevention and treatment can lower infection-related mortality and morbidity. Additionally, early treatment intervention can lower the number of deaths brought on by HIV and malaria. As a result, public health education is necessary to raise awareness within the population about HIV and malaria preventive and treatment measures as well as the effects of HIV and malaria coinfections.

Table 3: Parameter value and source.

Parameter	Value	Source
Λ_h	500/year	[1]
β_h	0.0001	Assumed
β_m	0.0002	Assumed
μ	0.02	[1]
δ_m	0.1	Assumed
η	0.1	[40]
ξ	0.1	[40]
δ_{am}	1	Assumed
δ_{hm}	0.1	Assumed
δ_a	1	[40]
Λ_v	50	Assumed
β_v	0.00015	Assumed
ν	0.001	Assumed
γ	0.1	Assumed
ω	0.1	Assumed
ρ	0.1	Assumed

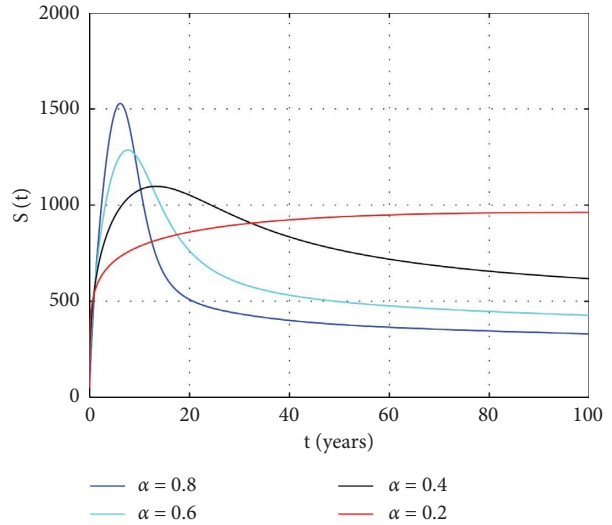

Figure 2: Numerical simulations of susceptible population size with different orders of fractional derivative.

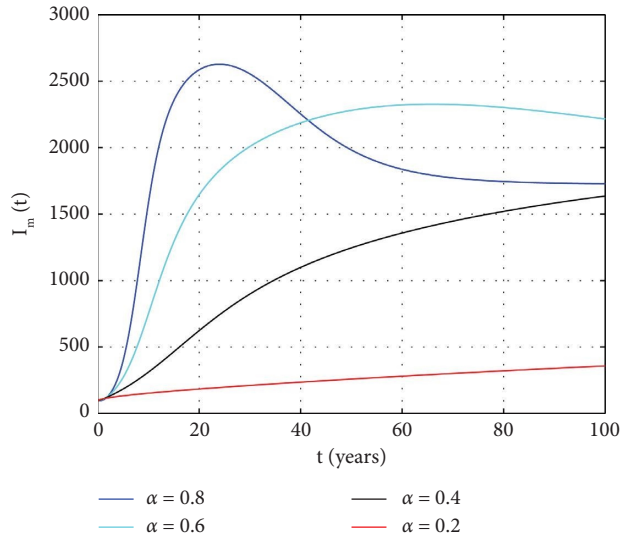

Figure 3: Numerical simulations of malaria infected human population size with different orders of fractional derivative.

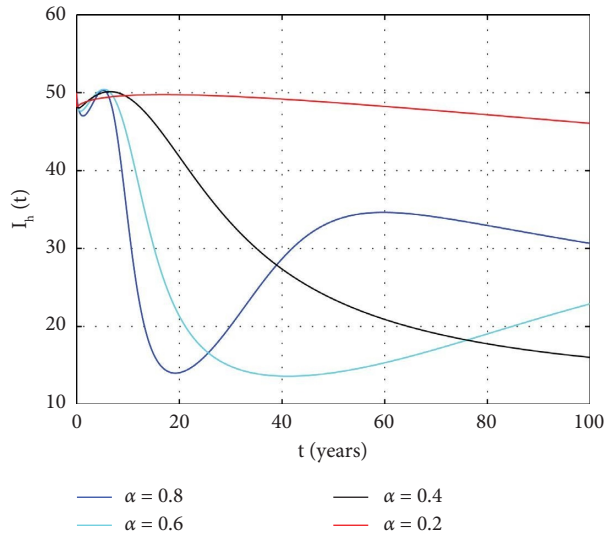

Figure 4: Numerical simulations of HIV infected human population size with different orders of fractional derivatives.

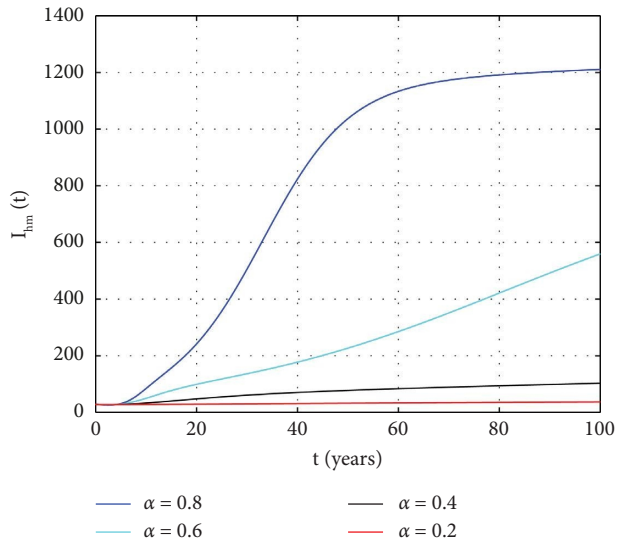

Figure 5: Numerical simulations of HIV-malaria infected human population size with different orders of fractional derivative.

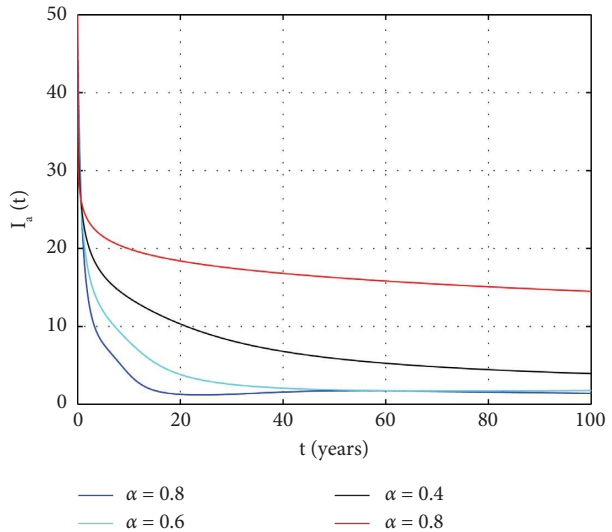

Figure 6: Numerical simulations of AIDS human population size with different orders of fractional derivative.

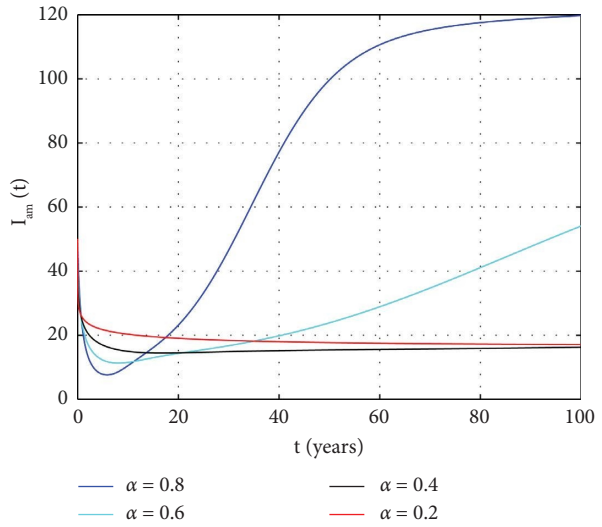

Figure 7: Numerical simulations of AIDS-malaria human population size with different orders of fractional derivative.

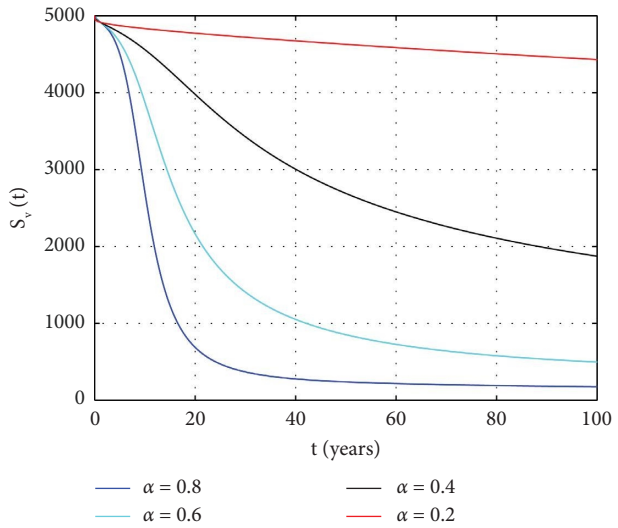

Figure 8: Numerical simulations of susceptible mosquito population size with different orders of fractional derivative.

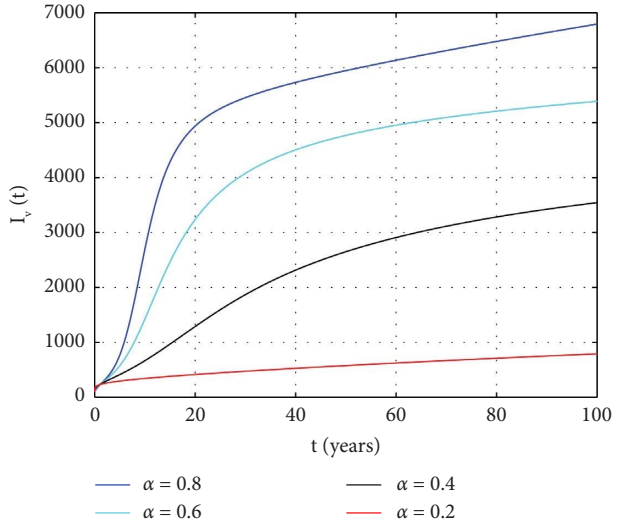

Figure 9: Numerical simulations of infected mosquito population size with different orders of fractional derivative.

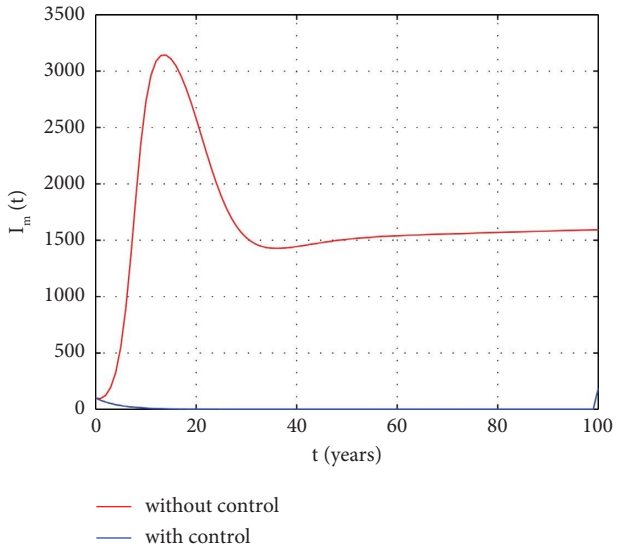

Figure 10: Numerical comparison of only malaria infected population size with and without applied controls.

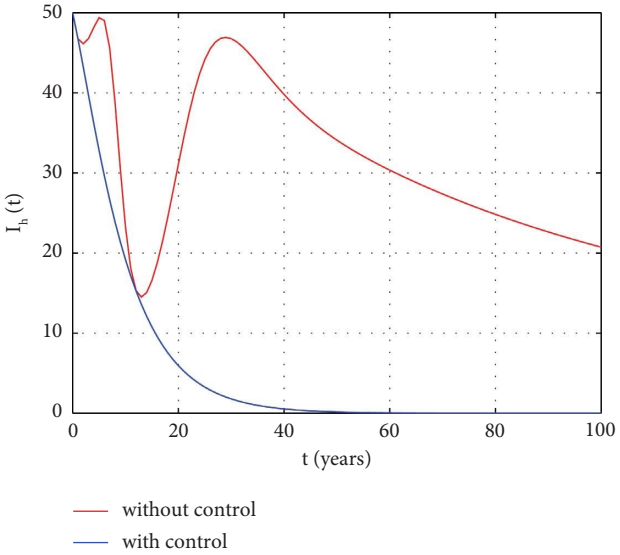

Figure 11: Numerical comparison of only HIV infected population size with and without applied controls.

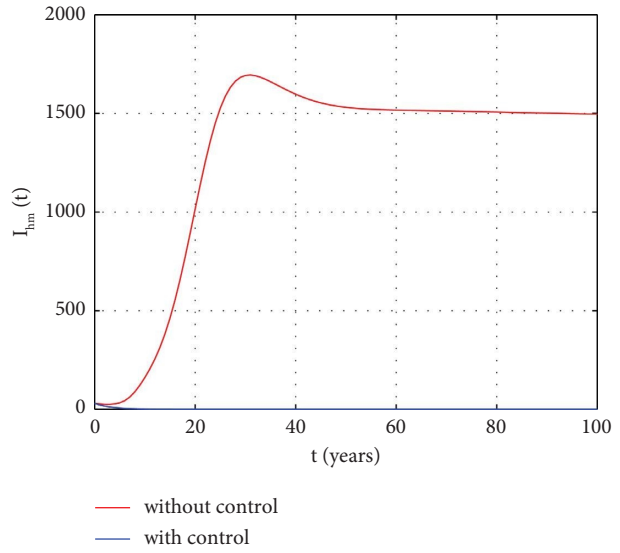

Figure 12: Numerical comparison of both malaria and HIV infected population size with and without applied controls.

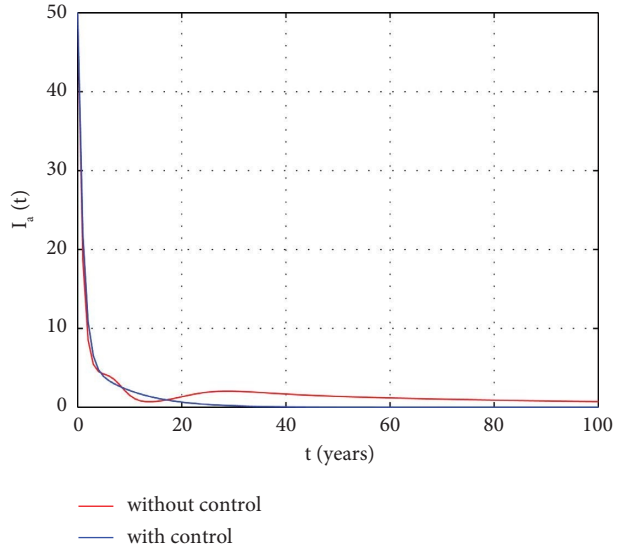

Figure 13: Numerical comparison of only AIDS stage population size with and without applied controls.

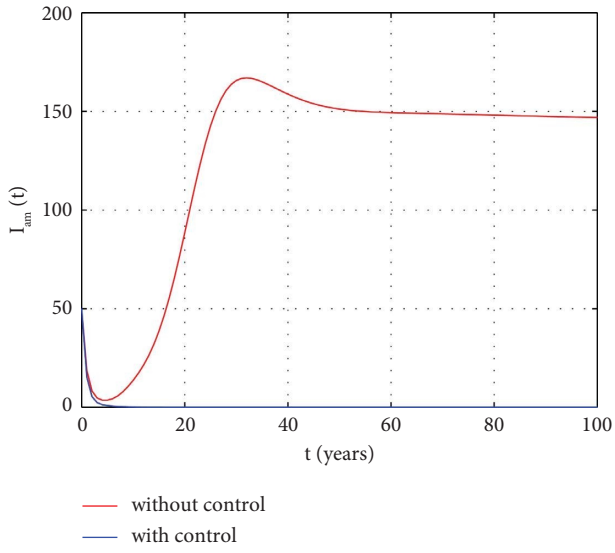

Figure 14: Numerical comparison of AIDS-malaria population size with and without applied controls.

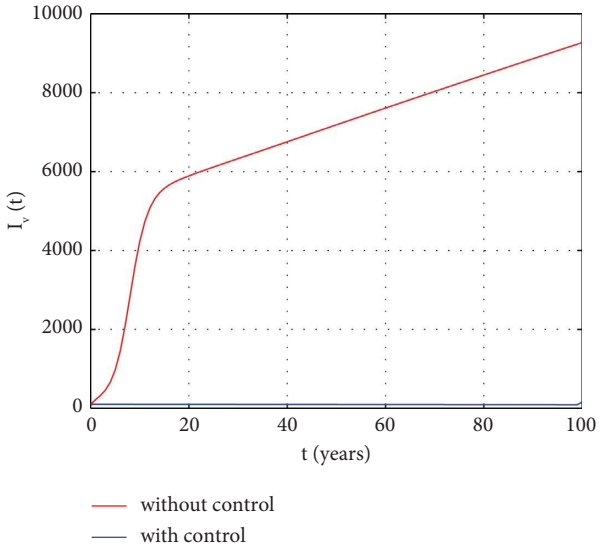

Figure 15: Numerical comparison of only infected mosquito population size with and without applied controls.

7. Conclusion

The high order of fractional derivative reduces the size of infected population at the beginning of the infection. Thus, early activation of population memory effects can reduce the size of infected population. On the other hand, the intervention with optimal control reduces the number of the infected population. Therefore, the results obtained from numerical simulations show that it is advisable to apply public health education for reducing the impact of HIV and malaria infections at the beginning or before the occurrence of infections whereas applying optimal control exhaustingly from the beginning to the entire period of infection reduces the impact of infections. [41–46].

Data Availability

All data used in the manuscript are included within the article.

Conflicts of Interest

The authors declare that they have no conflicts of interest.

References

[1] W. Fatmawati and L. Hanif, "Application of optimal control strategies to HIV-malaria co-infection dynamics," in *Journal of Physics: Conference Series*, vol. 974, no. 1, IOP Publishing, Bristol, UK, 2018.

[2] H.-F. Huo and G.-M. Qiu, "Stability of a mathematical model of malaria transmission with relapse," *Abstract and Applied Analysis*, vol. 2014, Article ID 289349, 9 pages, 2014.

[3] N. H. Sweilam, S. M. Al-Mekhlafi, Z. N. Mohammed, and D. Baleanu, "Optimal control for variable order fractional HIV/AIDS and malaria mathematical models with multi-time delay," *Alexandria Engineering Journal*, vol. 59, no. 5, pp. 3149–3162, 2020.

[4] H. Abboubakar, P. Kumar, N. A. Rangaig, and S. Kumar, "A malaria model with caputo–fabrizio and atangana–baleanu derivatives," *International Journal of Modeling, Simulation, and Scientific Computing*, vol. 12, no. 2, Article ID 2150013, 2021.

[5] J. Singh, D. Kumar, M. A. Qurashi, and D. Baleanu, "A new fractional model for giving up smoking dynamics," *Advances in Difference Equations*, vol. 2017, no. 1, pp. 88–16, 2017.

[6] B. Shiri and D. Baleanu, "Numerical solution of some fractional dynamical systems in medicine involving non-singular kernel with vector order," *Results in Nonlinear Analysis*, vol. 2, no. 4, pp. 160–168, 2019.

[7] R. Ross, "An application of the theory of probabilities to the study of a priori pathometry," *Proceedings of the Royal Society A*, vol. 92, pp. 204–230, 1916.

[8] J. Li, "Malaria model with stage-structured mosquitoes," *Mathematical Biosciences and Engineering*, vol. 8, no. 3, pp. 753–768, 2011.

[9] G. A. Ngwa and W. S. Shu, "A mathematical model for endemic malaria with variable human and mosquito populations," *Mathematical and Computer Modelling*, vol. 32, no. 7-8, pp. 747–763, 2000.

[10] N. Chitnis, J. M. Cushing, and J. M. Hyman, "Bifurcation analysis of a mathematical model for malaria transmission," *SIAM Journal on Applied Mathematics*, vol. 67, no. 1, pp. 24–45, 2006.

[11] N. Chitnis, D. Hardy, and T. Smith, "A periodically-forced mathematical model for the seasonal dynamics of malaria in mosquitoes," *Bulletin of Mathematical Biology*, vol. 74, no. 5, pp. 1098–1124, 2012.

[12] A. Boukhouima, K. Hattaf, and N. Yousfi, "A fractional order model for viral infection with cure of infected cells and humoral immunity," *International Journal of Differential Equations*, vol. 2018, Article ID 1019242, 12 pages, 2018.

[13] A. Boukhouima, K. Hattaf, E. M. Lotfi, M. Mahrouf, D. F. Torres, and N. Yousfi, "Lyapunov functions for fractional-order systems in biology: methods and applications," *Chaos, Solitons & Fractals*, vol. 140, Article ID 110224, 2020.

[14] K. Hattaf, "A new generalized definition of fractional derivative with non-singular kernel," *Computation*, vol. 8, no. 2, p. 49, 2020.

[15] Y. Wu, S. Ahmad, A. Ullah, and K. Shah, "Study of the fractional-order HIV-1 infection model with uncertainty in initial data," *Mathematical Problems in Engineering*, vol. 2022, Article ID 7286460, 16 pages, 2022.

[16] M. A. Dokuyucu and H. Dutta, "Analytical and numerical solutions of a TB-HIV/AIDS co-infection model via fractional derivatives without singular kernel," *Mathematical Modelling and Analysis of Infectious Diseases*, vol. 302, pp. 181–212, 2020.

[17] E. Okyere, F. T. Oduro, S. K. Amponsah, and I. K. Dontwi, "Fractional order optimal control model for malaria infection," 2016, https://arxiv.org/abs/1607.01612.

[18] P. Van den Driessche, "Reproduction numbers of infectious disease models," *Infectious Disease Modelling*, vol. 2, no. 3, pp. 288–303, 2017.

[19] K.-L. Li, J.-Y. Yang, and X.-Z. Li, "Competitive and exclusion and oscillation phenomena of an eco-epidemiological model: an invasive approach," *International Journal of Biomathematics*, vol. 16, no. 5, Article ID 2250103, 2023.

[20] J. Mushanyu, "A note on the impact of late diagnosis on HIV/AIDS dynamics: a mathematical modelling approach," *BMC Research Notes*, vol. 13, no. 1, p. 340, 2020.

[21] M. Marsudi, N. Hidayat, and R. Bagus Edy Wibowo, "Application of optimal control strategies for the spread of HIV in a population," *Research Journal of Life Science*, vol. 4, no. 1, pp. 1–9, 2017.

[22] S. Qureshi, A. Yusuf, A. A. Shaikh, M. Inc, and D. Baleanu, "Fractional modeling of blood ethanol concentration system with real data application," *Chaos: An Interdisciplinary Journal of Nonlinear Science*, vol. 29, no. 1, 2019.

[23] P. A. Naik, M. Yavuz, S. Qureshi, J. Zu, and T. Stuart, "Modeling and analysis of COVID-19 epidemics with treatment in fractional derivatives using real data from Pakistan," *The European Physical Journal Plus*, vol. 135, no. 10, p. 795, 2020.

[24] S. Qureshi and A. Yusuf, "Fractional derivatives applied to MSEIR problems: comparative study with real world data," *The European Physical Journal Plus*, vol. 134, no. 4, p. 171, 2019.

[25] S. D. Hove-Musekwa, F. Nyabadza, C. Chiyaka et al., "Modelling and analysis of the effects of malnutrition in the spread of cholera," *Mathematical and Computer Modelling*, vol. 53, no. 9-10, pp. 1583–1595, 2011.

[26] F. Ndaïrou, I. Area, J. J. Nieto, and D. F. M. Torres, "Mathematical modeling of COVID-19 transmission dynamics with a case study of Wuhan," *Chaos, Solitons & Fractals*, vol. 135, Article ID 109846, 2020.

[27] K. Sarkar, S. Khajanchi, and J. J. Nieto, "Modeling and forecasting the COVID-19 pandemic in India," *Chaos, Solitons & Fractals*, vol. 139, Article ID 110049, 2020.

[28] M. A. Khan, A. Atangana, E. Alzahrani, and Fatmawati, "The dynamics of COVID-19 with quarantined and isolation," *Advances in Difference Equations*, vol. 2020, no. 1, p. 425, 2020.

[29] P. Veeresha, H. M. Baskonus, D. Prakasha, W. Gao, and G. Yel, "Regarding new numerical solution of fractional Schistosomiasis disease arising in biological phenomena," *Chaos, Solitons & Fractals*, vol. 133, Article ID 109661, 2020.

[30] W. Gao, P. Veeresha, H. M. Baskonus, D. G. Prakasha, and P. Kumar, "A new study of unreported cases of 2019-nCOV epidemic outbreaks," *Chaos, Solitons & Fractals*, vol. 138, Article ID 109929, 2020.

[31] K. R. Cheneke, K. P. Rao, and G. K. Edessa, "Modeling and analysis of HIV and cholera direct transmission with optimal control," *Discrete Dynamics in Nature and Society*, vol. 2022, Article ID 5460337, 16 pages, 2022.

[32] W. Gao, P. Veeresha, D. G. Prakasha, H. M. Baskonus, and G. Yel, "New approach for the model describing the deathly disease in pregnant women using Mittag-Leffler function," *Chaos, Solitons & Fractals*, vol. 134, Article ID 109696, 2020.

[33] K. Regassa Cheneke, K. Purnachandra Rao, G. Kenassa Edesssa, and K. E. Gereme, "A new generalized fractional-order derivative and bifurcation analysis of cholera and human immunodeficiency co-infection dynamic transmission," *International Journal of Mathematics and Mathematical Sciences*, vol. 2022, Article ID 7965145, 15 pages, 2022.

[34] K. R. Cheneke, "Optimal control and bifurcation analysis of HIV model," *Computational and Mathematical Methods in Medicine*, vol. 2023, Article ID 4754426, 21 pages, 2023.

[35] H. M. Yang, "The basic reproduction number obtained from Jacobian and next generation matrices– a case study of dengue transmission modelling," *Biosystems*, vol. 126, pp. 52–75, 2014.

[36] O. Diekmann, J. A. P. Heesterbeek, and M. G. Roberts, "The construction of next-generation matrices for compartmental epidemic models," *Journal of The Royal Society Interface*, vol. 7, no. 47, pp. 873–885, 2010.

[37] O. Diekmann, J. A. P. Heesterbeek, and J. A. Metz, "On the definition and the computation of the basic reproduction ratio R 0 in models for infectious diseases in heterogeneous populations," *Journal of Mathematical Biology*, vol. 28, no. 4, pp. 365–382, 1990.

[38] F. Al Basir, K. B. Blyuss, and S. Ray, "Modelling the effects of awareness-based interventions to control the mosaic disease of Jatropha curcas," *Ecological Complexity*, vol. 36, pp. 92–100, 2018.

[39] M. Chen, R. Wu, Q. W. Zheng, and Q. Zheng, "Qualitative analysis of a diffusive COVID-19 model with NON-monotone incidence rate," *Journal of Applied Analysis & Computation*, vol. 13, no. 4, pp. 2229–2249, 2023.

[40] S. Rosa and D. F. M. Torres, "Numerical fractional optimal control of respiratory syncytial virus infection in octave/MATLAB," *Mathematics*, vol. 11, no. 6, p. 1511, 2023.

[41] H. Wang, H. Jahanshahi, M. K. Wang, S. Bekiros, J. Liu, and A. A. Aly, "A Caputo–Fabrizio fractional-order model of HIV/AIDS with a treatment compartment: sensitivity analysis and optimal control strategies," *Entropy*, vol. 23, no. 5, p. 610, 2021.

[42] F. S. Khan, M. Khalid, O. Bazighifan, and A. El-Mesady, "Euler's numerical method on fractional DSEK model under ABC derivative," *Complexity*, vol. 2022, Article ID 4475491, 12 pages, 2022.

[43] M. Helikumi, G. Eustace, and S. Mushayabasa, "Dynamics of a fractional-order chikungunya model with asymptomatic infectious class," *Computational and Mathematical Methods in Medicine*, vol. 2022, Article ID 5118382, 19 pages, 2022.

[44] E. M. Shaiful, E. M. Shaiful, and M. I. Utoyo, "A fractional-order model for HIV dynamics in a two-sex population,"

International Journal of Mathematics and Mathematical Sciences, vol. 2018, Article ID 6801475, 11 pages, 2018.

[45] A. A. M. Arafa, M. Khalil, and A. Sayed, "A non-integer variable order mathematical model of human immunodeficiency virus and malaria coinfection with time delay," *Complexity*, vol. 2019, Article ID 4291017, 13 pages, 2019.

[46] K. R. Cheneke, "Caputo fractional derivative for analysis of COVID-19 and HIV/AIDS transmission," in *Abstract and Applied Analysis*, vol. 2023, Hindawi, London, UK, 2023.